



Kinetics and thermodynamics of cyanide removal by ZnO@NiO nanocrystals

Mysam PIRMORADI¹, Saeedeh HASHEMIAN¹, Mohammad Reza SHAYESTE²

1. Department of Chemistry, Islamic Azad University, Yazd brunch, Yazd, Iran;

2. Department of Power and Electronic, Faculty of Engineering, Islamic Azad University, Yazd brunch, Yazd, Iran

Received 3 April 2016; accepted 1 October 2016

Abstract: ZnO, NiO and ZnO@NiO nanocrystals were successfully synthesized and characterized by FTIR, XRD and SEM methods. The average particles sizes of ZnO, NiO and ZnO@NiO were 32, 50 and 48 nm, respectively. The nanocrystals were examined as sensors for cyanide removal. The cyanide sensing test revealed that, compared with the pure ZnO, NiO, the ZnO@NiO nanocrystals exhibited highly improved sensing performances. The ZnO@NiO nano crystals were found to have better capacity for iron cyanide than sodium cyanide. The effects of significant parameters such as contact time, pH (2–12), nanocrystal dose (0.02–0.4 g) and cyanide concentration (5–50 mg/L) on the removal of cyanide by nanocrystals were explored. At an optimum pH<5, over 90% removal of 20 mg/L cyanide was obtained for nanocrystal dose of 0.2 g after 30 min contact time for iron cyanide by ZnO@NiO nano crystals. Cyanide removal was followed by pseudo second order kinetic model for ZnO@NiO nano crystals ($k_2=4.66\times 10^{-2}$ and $R^2=0.999$). The values of standard enthalpy change of 7.87 kJ/mol and standard free energy change of -18.62 kJ/mol at 298 K suggest the adsorption of cyanide on nanocrystals is an endothermic and spontaneous process. ZnO@NiO nanocrystal is an efficient sensor for removal of cyanide from water and wastewater.

Key words: cyanide removal; nano crystal; adsorption; ZnO@NiO

1 Introduction

Cyanides are discharged by various industries, chemical synthesis plants (nylon, fibers, resins, and herbicides), particularly in metallurgical processes, plating and surface finishing, heat treatment of steel, gold and base metals milling operations. They are a significant component of wastes from coke oven and blast furnace operations [1–3]. Electroplating industries are the most industrial sources of undesirable forms of cyanide ion wastewater. Cyanide compounds present in environmental matrices and waste streams as simple and complex cyanides, cyanates and nitriles [4]. Therefore, the wastewaters containing free and metal-complexed cyanides at different amounts are highly harmful to humans and aquatic organisms [5]. Cyanide has adverse health effects on people as well as other living organisms. The toxic effects of cyanide are so important to cause nerve damage and thyroid glands malfunctioning and established toxicity level so low (<0.1 mg/L). The acceptable level of cyanide at the effluent outlet lies between 4 and 40 $\mu\text{mol/L}$ [6]. To protect the environment and water bodies, wastewater containing cyanide must be

treated before discharging into the environment [6,7].

The removal of cyanide from wastewater by different methods such as ion-exchange and biodegradation was studied [8,9]. Although biodegradation is usually the preferred technique for treating wastewater due to its cost-effectiveness and environmental friendliness, there is little information on the use of bioprocesses for treatment of cyanide-laden wastewater. Cyanide is toxic to microorganisms, mainly in high concentrations, which leads to a low biodegradation rate and limits the probability of bioprocesses for efficiently eliminating cyanide and its compounds [10].

The electrochemical and chemical oxidation methods [11,12], ozonation [13] and coagulation [14,15] were widely investigated for the cyanide removal. However, these techniques are unattractive from both economic and environmental perspectives because they require the use of chemical compounds and do not degrade the full range of cyanide compounds [16]. Although, alkaline chlorination is widely used for the cyanide removal, it will lead to the formation of toxic cyanogens chloride and chloride disinfection by-products [17,18]. Advanced oxidation processes, e.g.

photochemical oxidation, ultrasonic waves for the treatment of cyanide effluents, have been also studied by some researchers. However, these are expensive, difficult to apply and not effective for the treatment of cyanides [11,19]. Among these methods, adsorption is an attractive process, in view of its efficiency and easiness. The adsorption is one of the suitable methods for the removal of cyanide ions with high removal efficiencies.

Adsorption is widely used for removal and recovery of cyanide [20,21]. Activated carbon is the most popular adsorbent for adsorption process due to its large surface area and high adsorption capacity as well as surface reactivity [22]. Activated carbon performs both as an adsorbent and as a catalyst for the oxidation of cyanide. Although its adsorptive properties were subjugated in most studies, activated carbon can act as an oxidation catalyst [23]. Activated carbon has low capacity for cyanide removal, consequently, production and regeneration of the activated carbon is very expensive, making it unreasonable for complete scale applications [10].

Several research groups used different types of adsorbents such as various agricultural products as adsorbent for the removal of cyanide from effluents [24]. The other agricultural waste materials sorbents such as banana peel [25], pistachio hull wastes [11], and rice husk [19] have been widely investigated for their ability to remove cyanide from water and wastewater.

Recently, nano transition metal oxide materials, like ZnO, CuO and NiO, have attracted intense interest, because these metal oxides are a nontoxic, green synthesis, inexpensive and non-hygroscopic powder. Therefore, some of metal oxides were used as sorbent / catalyst for cyanide removal [26,27]. Zinc oxide is a versatile material that has achieved applications in photocatalysts, solar cells, chemical sensors, piezoelectric transducers and transparent electrodes. Zinc oxide, which is an n-type semiconductor with a wide band gap and a biosafe and biocompatible material, has attracted a significant research interest due to its unique properties and wide applications in transparent electronics, piezoelectric devices, chemical and biological sensing, and catalytic reactions [28–30]. A NiO/ZnO hybrid nanoparticle was used for electrochemical sensing of dopamine and uric acid [31], xylene sensors [32] and for CO optical sensing [33]. NiO@ZnO heterostructure was also used as gas sensing [34].

This work aimed to prepare NiO, ZnO and NiO@ZnO nanocrystals. The second pursue of this work is cyanide sensing by NiO, ZnO and NiO@ZnO nanocrystals. Thus, a set of experiments were carried out to study the capacity of nanocrystals to remove cyanide under varying conditions. The influences of solution pH,

adsorbent dose, cyanide concentration and contact time on cyanide adsorption were evaluated. The kinetics and thermodynamics of the cyanide adsorption process were also analyzed.

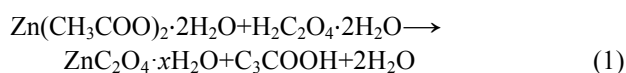
2 Experimental

2.1 Materials and methods

All of the chemicals were purchased from Merck Chemical Co. All of compounds were analytical grade and were used as-received without any purification. Sodium cyanide (NaCN) and potassium hexacyano ferrate ($K_4[Fe(CN)_6]$ -iron cyanide) as sources of cyanide were used. The 1000 mg/L stock solution of cyanide was prepared and all the solutions used in the experiments were prepared by diluting the stock solution with double distilled water to the desired concentrations. UV-Vis spectrophotometer 160A Shimadzu was used for determination of concentration of cyanide. IR measurements were performed by FTIR tensor-27 of Burker Co., using the KBr pellet between the ranges 400 to 4000 cm^{-1} . The powder X-ray diffraction studies were made on a Siemens, D5000 (Germany) diffractometer using Ni-filtered $Cu K_{\alpha}$ radiation and wavelength 1.54 Å. The average particle size and morphology of samples were observed by SEM using a Hitachi S-3500 scanning electron microscope. All pH measurements were carried out with an ISTEK-720P pH meter.

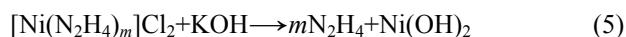
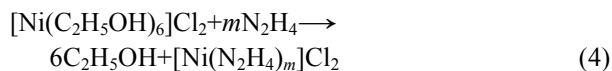
2.2 Preparation of nanocrystals

Zinc oxide was synthesized in aqueous solutions by using zinc acetate and oxalic acid under hydrothermal conditions. Zinc acetate solution (0.1 mol/L) and oxalic acid solution (0.1 mol/L) were stirred for about 12 h. The white precipitates thus obtained are filtered and washed with distilled water and acetone to remove impurities and dried over 120 °C for 5 h in order to remove water molecules. The calcination process was carried out over a temperature of 400–450 °C in order to remove CO and CO₂ from the compound [35].



Nickel oxide has been successfully synthesized by the chemical reduction of nickel chloride with hydrazine at room temperature and thermal decomposition of Ni(OH)₂ without any protective agent and inert gas protection. Nickel chloride hexa hydrate (0.111 mol/L) in ethanol was used as precursors, and was added to hydrazine monohydrate solution (6.73 mL). The pH was adjusted from 8.0 to 12 using potassium hydroxide. The reaction was stirred for 2 h at room temperature. The resultant product was washed thoroughly with deionized

water for removal of reaction residues followed by washing with acetone. Finally, deep green nanocrystals $[\text{Ni}(\text{OH})_2 \cdot 0.5\text{H}_2\text{O}]$ were formed and dried [36]. The $\text{Ni}(\text{OH})_2$ nanocrystals were converted to NiO by thermal decomposition at 500 °C. During the synthesis of NiO nanocrystals, the following reactions are reasonable:



For the synthesis of coupled ZnO and NiO (ZnO@NiO), zinc acetate and nickel chloride in 1:1 molar ratio were dissolved in deionized water and mixed with required amount of an oxalic acid solution (0.1 mol/L) are stirred and treated in a microwave oven to synthesize coupled metal oxide of ZnO@NiO .

2.3 Adsorption studies

In order to study the effect of different parameters such as the contact time, pH, and sorbent dosage on the sorption, various experiments were carried out by agitation of known amount of sorbents (0.1 g) in 50 mL of cyanide solution with an initial concentration of 20 mg/L on rotary shaker at a constant speed of 150 r/min at room temperature (25 °C). The effect of pH was studied by adjusting the pH of solutions in the range of 2–12 with 0.1 mol/L NaOH or HCl solutions. To evaluate the adsorption thermodynamic parameters, the effect of temperature on adsorption was studied at 15–60 °C.

Each experiment was repeated five times, and the average results were given. Relative standard deviation (% RSD) was determined between 1.82%–3.1% for each point at all the experiments.

The removal rate of cyanide by the ZnO, NiO and ZnO@NiO sorbents is given by

$$\eta = (C_0 - C_e) / C_0 \times 100\% \quad (7)$$

where C_0 and C_e are denoted the initial and equilibrium concentration (mg/L) of cyanide respectively. The amount of cyanide adsorbed (q_e) was determined by using the following equation:

$$q_e = (C_0 - C_e)V/m \quad (8)$$

where V is the volume of the solutions (mL) and m is the amount (mg) of nanocrystals.

3 Results and discussion

3.1 Characterization of ZnO, NiO and ZnO@NiO

The XRD patterns of the ZnO, NiO and ZnO@NiO are given in Fig. 1. For ZnO, the diffraction peaks are

located at $2\theta = 33.5^\circ$, 36° and 38° , which are associated with (110), (112) and (101), and this pattern has been indexed as hexagonal phase of ZnO (JPCDS card No. 36-1451). The observed diffraction peaks of NiO at $2\theta = 33^\circ$, 38° , 43° are associated with (311), (111) and (200) planes, respectively [37,38] with face-centered cubic (FCC) crystal pattern and lattice constant $a = 3.85 \text{ \AA}$. This pattern has been indexed as FCC phase of NiO (JPCDS card No. 78-0643) [36]. It was seen that the lattice constants of ZnO@NiO solid solution were between those of two end materials ZnO (JPCDS No. 36-1451) and cubic phase of NiO (JPCDS card No. 78-0643), confirming the formation of ZnO@NiO nanocrystals solid solution (JPCDS card No. 04-0835).

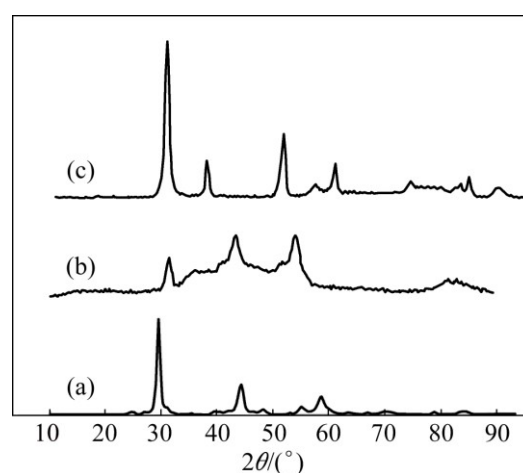


Fig. 1 XRD patterns of ZnO (a), NiO (b) and ZnO@NiO (c) nanocrystals

The XRD pattern shows that the samples had other distinct impurity diffraction peak in addition to the characteristic peaks of FCC phase ZnO and ZnO@NiO . The impurities may be oxalate ions for preparation of ZnO and ZnO@NiO nanocrystals.

The crystallite sizes of the nanocrystals were calculated using the Scherrer's formula:

$$D = K\lambda / (\beta \cos \theta) \quad (9)$$

where D is taken as crystallite size, K is a constant which equals to 0.9, λ is 1.5406 Å, β is the FWHM measured in radians on the 2θ scale, θ is the Bragg angle for the diffraction peaks.

The average crystallite sizes of ZnO and NiO were 30–40 nm, 45–55 nm, respectively, which were derived from the FWHM of the most intense peak. For the coupled metal oxides (ZnO@NiO) the average crystallite size was 40–50 nm.

The surface morphology and size of the as-prepared ZnO, NiO and coupled metal oxide ZnO@NiO were examined by SEM. SEM image of ZnO shows that the particles were nearly of flower shape (Fig. 2(a)). The

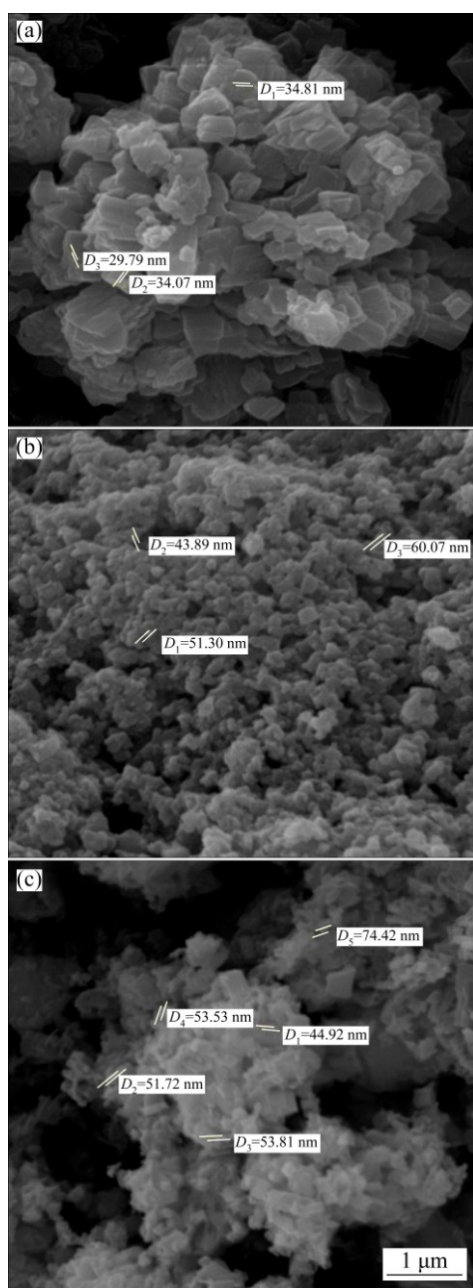


Fig. 2 SEM images of ZnO (a), NiO (b) and ZnO@NiO (c) nanocrystals

figure clearly indicates the morphology of the particles to be roughly spherical and homogeneous. Figure 2(b) shows the SEM image of NiO nanoparticles, which are spherical. Figure 2(c) shows the SEM image of the coupled metal oxide (ZnO@NiO) nanocrystals. In the coupled metal oxide (ZnO@NiO), NiO nano spheres are embedded in the matrix of ZnO nano particles. The SEM images show that the particles are also aggregated.

The composition of the as-prepared ZnO, NiO and coupled metal oxide ZnO@NiO was analyzed by means of energy dispersive X-ray analysis (EDX) as shown in Table 1. The EDX result showed the presence of Zn and O, Ni and O, and Zn, Ni, O and some impurities such as

C (from oxalate), respectively. The results showed peaks corresponding to zinc, nickel and oxygen, and therefore, the formation of ZnO@NiO is also confirmed by using EDX analysis.

Table 1 Composition of elements in ZnO, NiO and ZnO@NiO

Nanocrystal	Mole fraction/%				
	Zn	O	Ni	C	N or Cl
ZnO	48.2	47	–	4.3	Trace
NiO	–	48.80	49.2	1.6	Trace
ZnO@NiO	24.1	46.	24.6	3.2	2

The FTIR absorption spectra of ZnO, NiO and ZnO@NiO are shown in Figs. 3–5, respectively. The broad absorption peaks around $3400\text{--}3500\text{ cm}^{-1}$ and $1620\text{--}1640\text{ cm}^{-1}$ are attributed to O–H stretching and H–O–H bending vibration of H_2O . The broad absorption bands in the region of $400\text{--}850\text{ cm}^{-1}$ are assigned to M–O (M=Zn, Ni) stretching vibration mode; the broadness of the absorption band indicates that the M–O powders are nanocrystals [39]. The sharp and intense peaks observed at $2000\text{--}2200\text{ cm}^{-1}$ are assigned to the bending vibration of cyanide [40,41].

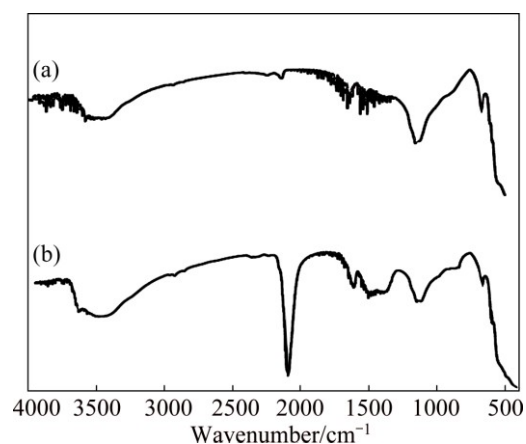


Fig. 3 FTIR spectra of ZnO (a) and ZnO adsorbed cyanide (b)

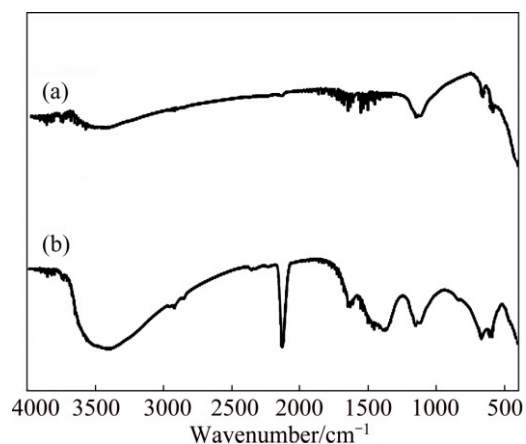


Fig. 4 FTIR spectra of NiO (a) and NiO adsorbed cyanide (b)

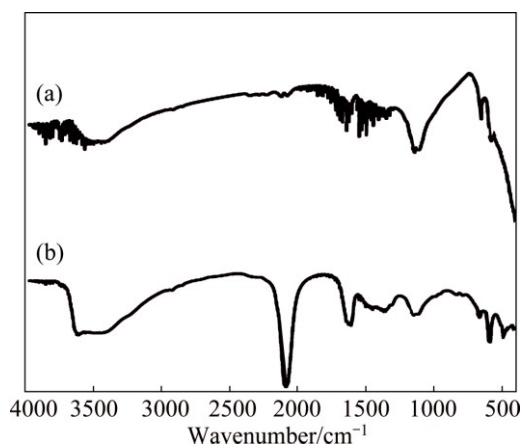


Fig. 5 FTIR spectra of ZnO@NiO (a) and ZnO@NiO adsorbed cyanide (b)

3.2 Sensing activity toward cyanide

The sensing property of ZnO, NiO and ZnO@NiO nanocrystals for cyanide was investigated. Accordingly, the adsorption activities of ZnO, NiO and ZnO@NiO nanocrystals as sorbent and cyanides (NaCN and $K_4[Fe(CN)_6]$) as the model of pollutant at different conditions such as contact time, pH and mass of nanocrystals were evaluated.

3.2.1 Effect of contact time

The contact time between the pollutant and the adsorbent is of significant importance in the wastewater treatment by adsorption. The effect of contact time (0–180 min) was studied for removal of cyanide from aqueous solution.

Figures 6 and 7 show the plot of removal rate of cyanide against contact time for ZnO, NiO and ZnO@NiO nanocrystals at adsorbent mass of 0.1 g. It was observed from Figs. 6 and 7 that the rate of cyanide removal was rapid for iron cyanide, but the process was slower for sodium cyanide. For the iron cyanide compounds the equilibrium condition was reached at the first 30 min of contact time, but for sodium cyanide compound the equilibrium condition was achieved only after 120 min. The maximum rate of cyanide removal reached 60% for sodium cyanide and 88% for iron cyanide at these periods. The slow step in the sodium cyanide solution was considered to be the diffusion of cyanide from the bulk solution to the active surface sites. The strong chemical binding of adsorbates with adsorbent requires a longer contact time for the attainment of equilibrium, but in physical adsorption most of the adsorbates species are adsorbed within a short interval of contact time. However, available adsorption results reveal that the uptake of adsorbate species was fast at the initial stage of contact time, and thereafter, it becomes slower near the equilibrium.

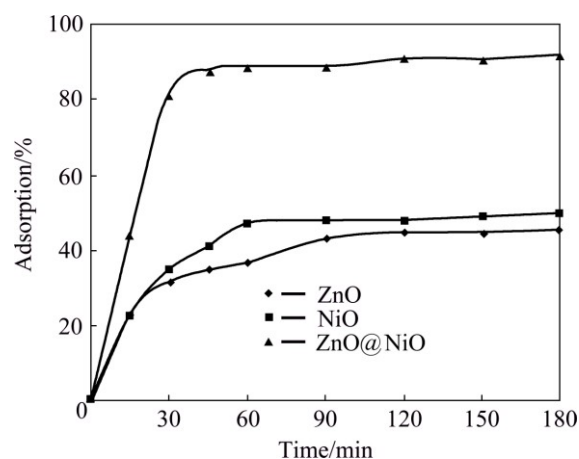


Fig. 6 Effect of contact time for adsorption of iron cyanide onto ZnO, NiO and ZnO@NiO nanocrystals

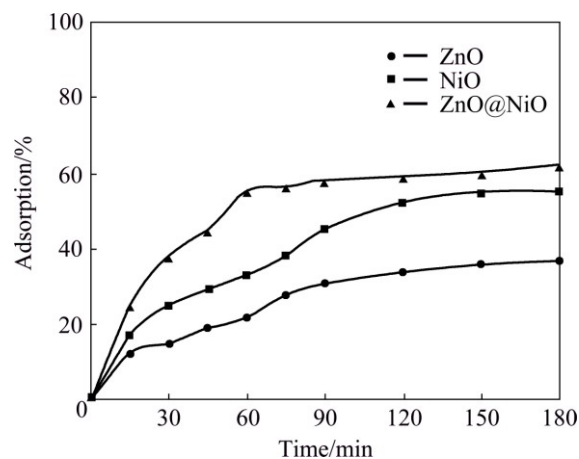


Fig. 7 Effect of contact time for adsorption of sodium cyanide onto ZnO, NiO and ZnO@NiO nanocrystals

3.2.2 Effect of initial pH

Effect of pH of media on sensing property of cyanide by ZnO, NiO and ZnO@NiO nanocrystals was investigated. Figure 8 shows that pH plays an important role in the adsorption process of cyanide by ZnO, NiO and ZnO@NiO nanocrystals. The results show that as the pH increases up to 5 the adsorption of cyanide will be less favorable. It is due to the electrostatic repulsion between the adsorptive anion and the surface of the nanocrystals that gradually become more negatively charged [13]. The acidic medium (pH 2–3) is desirable for the adsorption process of cyanide.

3.2.3 Effect of initial concentration

The effect of initial concentration of cyanide was investigated from 2–30 mg/L. The results showed that using the adsorbent material, the removal rate of cyanide was first increased from 2–20 mg/L, and then decreased when the initial concentration of cyanide was increased (20–30 mg/L) at constant other variables. This can be explained by the fact that the initial concentration of cyanide had a restricted effect on the cyanide removal

capacity; simultaneously, the adsorbent media had a limited number of active sites, which would have become saturated at a certain concentration. This leads to the increase in the number of cyanide molecules competing for the available functions groups on the surface of adsorbent material. Since the solution of lower concentration has a small amount of cyanide than the solution of higher concentration, the removal rate was decreased with increasing initial concentration of cyanide [42].

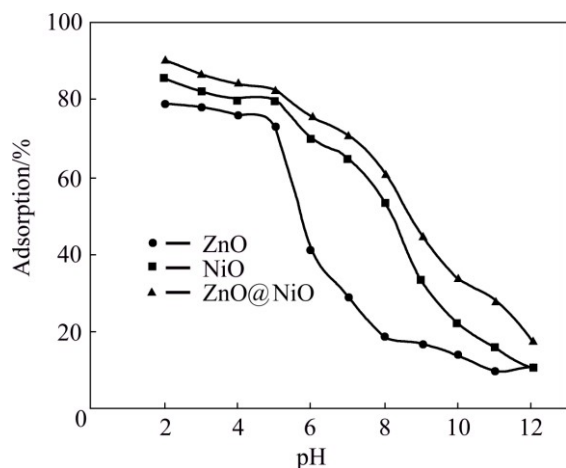


Fig. 8 Effect of pH on cyanide removal by ZnO, NiO and ZnO@NiO nanocrystals

3.2.4 Effect of dosage of ZnO, NiO and ZnO@NiO

Effect of nanocrystal dosage for cyanide sensing was investigated. The removal rate of cyanide increased with the dosage increasing from 0.02–0.2 g of nanocrystals. Although the removal rate increased with the increase in adsorbent dosage, but above 0.2 g, it did not show significant effect for uptake of cyanide on nanocrystals. The increase in the rate of cyanide removal from the aqueous solution is due to the greater number of active sites available for adsorption [43].

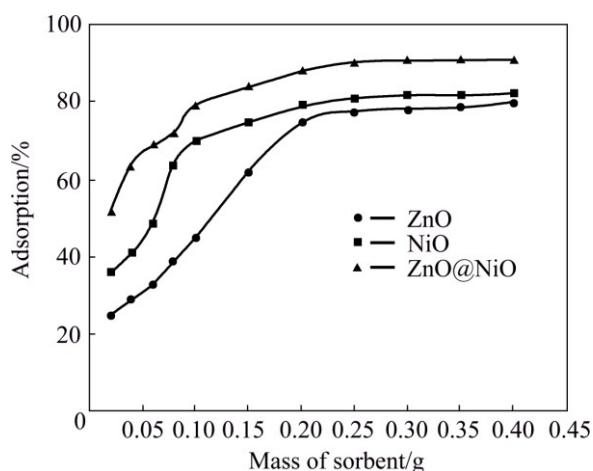


Fig. 9 Effect of adsorbent dosage on adsorption of cyanide by ZnO, NiO and ZnO@NiO

3.3 Kinetics of cyanide adsorption onto ZnO, NiO and ZnO@NiO

The adsorption kinetic experiments were carried out to evaluate the rate of sorption process on the ZnO, NiO and ZnO@NiO nanocrystals. The kinetic data of adsorption can be evaluated using different types of mathematical models. The brief behavior of cyanide adsorption process was analyzed by using the pseudo-first order and pseudo-second order kinetic models [44–46]. The pseudo-first order model assumes that the rate of change of solute uptake with time is directly proportional to difference in saturation concentration and amount of solid uptake with time:

$$\ln(q_e - q_t) = \ln q_e - k_1 t \quad (10)$$

where q_e and q_t are the amounts of cyanide adsorbed per unit mass of the nanocrystals (mg/g) at equilibrium and time t , respectively, and k_1 is the rate constant of adsorption (min^{-1}). When $\ln(q_e - q_t)$ was plotted against time, a straight line should be obtained with a slope of k_1 if the first order kinetics is valid.

The pseudo-second order model has the following form:

$$t/q_t = t/q_e + 1/(k_2 q_e^2) \quad (11)$$

where k_2 is the rate constant of the pseudo-second order equation ($\text{g} \cdot \text{mg}^{-1} \cdot \text{min}^{-1}$). A plot of t/q_t versus time (t) would yield a line with a slope of $1/q_e$ and an intercept of $1/(k_2 q_e^2)$ if the second order model is a suitable expression. The kinetic model with a higher correlation coefficient R^2 was selected as the most suitable one (Figs. 10 and 11). It was found that the application of pseudo-second-order kinetic model for adsorption of cyanide by ZnO@NiO nanocrystals provides better correlation coefficient of experimental data (Table 2).

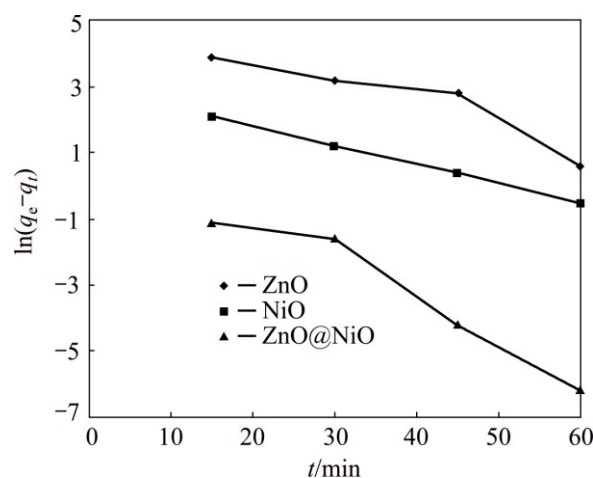


Fig. 10 Pseudo-first-order kinetic for adsorption of cyanide onto ZnO, NiO and ZnO@NiO nanocrystals (30 mL cyanide solution, 20 mg/L initial concentration, initial pH 3.0, and 0.2 g nanocrystal)

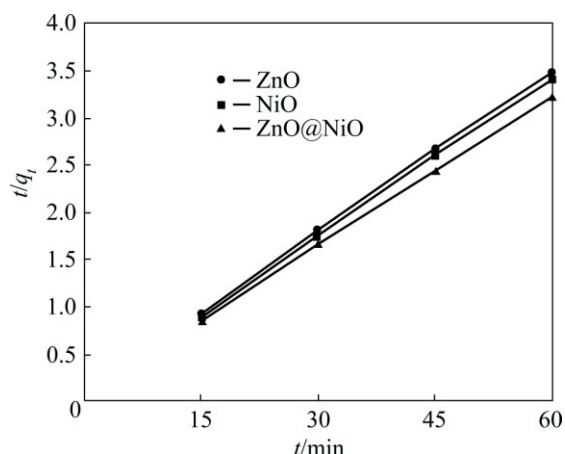


Fig. 11 Pseudo-second-order kinetic for adsorption of cyanide onto ZnO, NiO and ZnO@NiO nanocrystals (30 mL cyanide solution, 20 mg/L initial concentration, initial pH 3.0, and 0.2 g nanocrystal)

Table 2 Kinetic parameters for cyanide removal by ZnO, NiO and ZnO@NiO nanocrystals

Nanocrystal	First order		Second order	
	R^2	k_1/min^{-1}	R^2	$k_2/(\text{g}\cdot\text{mg}^{-1}\cdot\text{min}^{-1})$
ZnO	0.871	6.87×10^{-2}	0.942	4.06×10^{-2}
NiO	0.999	5.76×10^{-2}	0.995	6.27×10^{-2}
ZnO@NiO	0.94	1.4×10^{-2}	0.999	4.66×10^{-2}

3.4 Thermodynamic study

The thermodynamic parameters are the actual indicators for practical application of a process [47]. The amount of cyanide adsorbed at equilibrium at different temperatures (15–60 °C), was examined to obtain thermodynamic parameters for the adsorption system. The thermodynamic parameters, change in the standard free energy (ΔG^\ominus), enthalpy (ΔH^\ominus) and entropy (ΔS^\ominus), associated with the adsorption process were determined using the following equations [48]:

$$\Delta G^\ominus = -RT \ln K_C \quad (12)$$

where ΔG^\ominus is the standard free energy change, R is the universal gas constant ($8.314 \text{ J}\cdot\text{mol}^{-1}\cdot\text{K}^{-1}$), T is the absolute temperature and K_C is the equilibrium constant. The apparent equilibrium constant of the sorption, K_C , is obtained from

$$K_C = C_A/C_S \quad (13)$$

where K_C is the equilibrium constant, C_A is the amount of cyanide adsorbed on the nanocrystals at equilibrium (mg/L) and C_S is the equilibrium concentration of cyanide in the solution (mg/L). K_C values were calculated at different temperatures for determination of thermodynamic equilibrium constant (K_C) [49]. The free energy changes are also calculated by using the

following equation:

$$\ln K_C = -\Delta G^\ominus/(RT) = -\Delta H^\ominus/(RT) + \Delta S^\ominus/R \quad (14)$$

ΔH^\ominus and ΔS^\ominus were calculated from the slope and intercept of vant Hoff plots of $\ln K_C$ versus $1/T$ (Fig. 12). The results are given in Table 3.

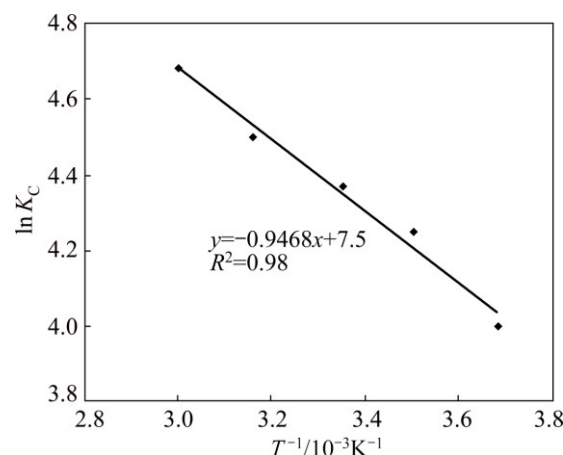


Fig. 12 Plot of $\ln K_C$ vs $1/T$ (30 mL cyanide solution, 20 mg/L initial concentration, initial pH 3.0, and 0.2 g nanocrystal)

Table 3 Thermodynamic parameters of cyanide removal by ZnO@NiO nanocrystals

$T/^\circ\text{C}$	$\Delta G^\ominus/(\text{kJ}\cdot\text{mol}^{-1})$	$\Delta H^\ominus/(\text{J}\cdot\text{mol}^{-1})$	$\Delta S^\ominus/(\text{J}\cdot\text{mol}^{-1}\cdot\text{K}^{-1})$
15	-18		
20	-18.3		
25	-18.62		
30	-7.87	7.87	62.52
40	-19.56		
50	-20.18		
60	-20.8		

The negative ΔG^\ominus values indicated thermodynamically feasible and spontaneous nature of the adsorption of cyanide. The decrease in negative ΔG^\ominus values with increasing temperatures shows an increase in feasibility of sorption at higher temperatures. The ΔH^\ominus parameter was found to be $7.87 \times 10^{-3} \text{ kJ/mol}$.

The positive ΔH^\ominus and ΔS^\ominus (Table 3) reveal that the adsorption was endothermic and the disorder of the cyanide was increased by the adsorption process. The positive ΔS^\ominus also shows the increase in randomness at the solid/solution interface with some structural changes during the fixation of cyanide on the active sites of the ZnO@NiO nanocrystal [50].

3.5 Isotherm study

The isotherm study would be informative for determining the maximum capacity of nanocrystals for adsorbing cyanide. An isotherm represents the

relationship between the amount of cyanide adsorbed by nanocrystals at given experimental conditions and the equilibrium concentration of cyanide in the liquid phase. To simulate the adsorption isotherm, two commonly used models, the Langmuir and Freundlich isotherms, were employed [51]. The Langmuir equation can be written in the following form:

$$C_e/q_e = (1/q_{\max}k_L) + C_e/q_{\max} \quad (15)$$

where q_e is the solid phase equilibrium concentration (mg/g); C_e is the liquid equilibrium concentration of cyanide in solution (mg/L); k_L is the equilibrium adsorption constant related to the affinity of binding sites (mg^{-1}); and q_{\max} is the maximum amount of cyanide per unit mass of adsorbent for complete monolayer coverage.

The Freundlich isotherm describes adsorption where adsorbent has a heterogeneous surface with adsorption sites that have different energies of adsorption. The energy of adsorption varies as a function of the surface coverage (q_e) and is represented by the Freundlich constant K_F ($\text{mg} \cdot \text{g}^{-1}$).

$$q_e = K_F C_e^{1/n} \quad (16)$$

$$\lg q_e = \lg K_F + (1/n) \lg C_e \quad (17)$$

where K_F is roughly an indicator of the adsorption capacity and n is the heterogeneity factor which has a lower value for more heterogeneous surfaces.

Results from the Langmuir and Freundlich analysis of the adsorption of cyanide on the nanocrystals are reported in Table 4. The fitting curves and correlation coefficient values both indicate that the Langmuir model describes better the adsorption onto nanocrystals.

Table 4 Langmuir and Freundlich constants for adsorption of cyanide by nanocrystals

Sorbent	Freundlich			Langmuir		
	$K_F/$ ($\text{mg} \cdot \text{g}^{-1}$)	n	R^2	$q_m/$ ($\text{mg} \cdot \text{g}^{-1}$)	$K_L/$ ($\text{L} \cdot \text{mg}^{-1}$)	R^2
ZnO	3.2	0.92	0.824	275	2.5×10^{-4}	0.996
NiO	2.55	0.85	0.815	185	2.95×10^{-3}	0.994
ZnO@NiO	2.4	0.91	0.79	320	3.2×10^{-3}	0.999

3.6 Comparison of nanocrystals with other sorbents

The kinetic model and adsorption capacity of cyanide onto ZnO, NiO and ZnO@NiO nanocrystals were compared with various adsorbents. The ZnO, NiO and ZnO@NiO nanocrystals of this study have reasonable adsorption capacity in comparison with other sorbents. Adsorption parameters of different sorbents for cyanide were compared and reported in Table 5.

3.7 Regeneration study

The stability of the ZnO@NiO nanocrystals as adsorbent was investigated by regeneration experiments.

The physical regeneration of ZnO@NiO nanocrystal was done by heating at 100–400 °C. The regeneration temperature was at 300 °C. The temperature higher than 300 °C did not have significant effect on the regeneration efficiency of ZnO@NiO nanocrystal. Generally, the adsorption capacity of the ZnO@NiO nanocrystal decreases as the number of regeneration cycle increases from 3 to 5. The adsorption capacity of the ZnO@NiO nanocrystal for cyanide did not show any significant decrease even after 2 regenerations. After 3 cycles 75% and after 5 cycles 54% of cyanide was removed. The value of cycles corresponds to the adsorption capacity of the original nanocrystal. The ZnO@NiO nanocrystal is simple to thermally regenerate. The good regeneration results and relatively low regeneration temperature demonstrated that the ZnO@NiO nanocrystal could offer high sensing property for removal of cyanide.

Table 5 Comparison of adsorption parameters of cyanide with different sorbents

Sorbent	Kinetic	$q_{\max}/$ ($\text{mg} \cdot \text{g}^{-1}$)	Ref.
Ag-activated carbon	–	16.426	[3]
Pistachio hull wastes	Pseudo-second-order	156.2	[10]
Activated carbon		7673.2	[52]
Alumina	–	221.97	[52]
Cu-activated carbon	Pseudo-second-order	297.2	[52]
Bone charchol	Pseudo-second-order	140	[53]
Date stones	Pseudo-second-order	50.21	[54]
Alumina	–	62.5	[55]
SBA	Both pseudo-first order and pseudo second order	4.43	[56]
ZnO	Pseudo-second-order	275	In this study
NiO	Pseudo- first -order	185	In this study
ZnO@NiO	Pseudo-second-order	320	In this study

4 Conclusions

The ZnO, NiO and ZnO@NiO nanocrystals were prepared and characterized. The nanocrystals were used as cyanide sensing. The sodium cyanide and iron cyanide as source of cyanide were examined. The iron cyanide had higher sensing to nanocrystals at acidic conditions ($\text{pH} < 5$). The adsorption of cyanide onto nanocrystals was followed by pseudo second order kinetic model and Langmuir isotherm model.

Acknowledgments

We gratefully acknowledge financial support from the Research Council of Islamic Azad University of Yazd.

References

- [1] AKCIL A, MUDDER T. Microbial destruction of cyanide wastes in gold mining: Process review [J]. *Biotechnology Letters*, 2003, 25: 445–450.
- [2] KUYUCAK N, AKCIL A. Cyanide and removal options from effluents in gold mining and metallurgical processes [J]. *Minerals Engineering*, 2013, 50: 13–29.
- [3] DEVECI H, YAZICI E Y, ALP I, USLU T. Removal of cyanide from aqueous solutions by plain and metal-impregnated granular activated carbons [J]. *International Journal of Mineral Processing*, 2006, 79: 198–208.
- [4] PAPANITRIOU C A, SAMARAS P, SAKELLAROPOULOS G P. Comparative study of phenol and cyanide containing wastewater in CSTR and SBR activated sludge reactors [J]. *Bioresource Technology*, 2009, 100: 31–37.
- [5] PATIL Y B, PAKNIKAR K M. Development of a process for bio detoxification of metal cyanides from wastewater [J]. *Process Biochemistry*, 2000, 35: 1139–1151.
- [6] DASHA R, BALOMAJUMDER C, KUMAR A. Removal of cyanide from water and wastewater using granular activated carbon [J]. *Chemical Engineering Journal*, 2009, 146: 408–413.
- [7] ADHOUM N, MONSER L. Removal of cyanide from aqueous solution using impregnated activated carbon [J]. *Chemical Engineering and Processing: Process Intensification*, 2002, 41: 17–21.
- [8] DAI X, BREUER P L, JEFFREY M I. Comparison of activated carbon and ion-exchange resins in recovering copper from cyanide leach solutions [J]. *Hydrometallurgy*, 2010, 101: 48–57.
- [9] GUPTA A, JOHNSON E F, SCHLOSSEL R H. Investigation into the ion exchange of the cyanide complexes of zinc²⁺, cadmium²⁺, and copper¹⁺ ions [J]. *Industrial Engineering Chemistry Research*, 1987, 26: 588–594.
- [10] MOUSSAVI G, KHOSRAVI R. Removal of cyanide from wastewater by adsorption onto pistachio hull wastes: Parametric experiments, kinetics and equilibrium analysis [J]. *Journal of Hazardous Materials*, 2010, 183: 724–730.
- [11] TIAN Shi-chao, LI Yi-bing, ZHAO Xu. Cyanide removal with a copper/active carbon fiber cathode via a combined oxidation of a Fenton-like reaction and in situ generated copper oxides at anode [J]. *Electrochimica Acta*, 2015, 180: 746–755.
- [12] SZPYRKOWICZ L, ZILIOGRANDI F, KAUL S, RIGONISTERN S. Electrochemical treatment of copper cyanide wastewaters using stainless steel electrodes [J]. *Water Science and Technology*, 1998, 38: 261–268.
- [13] BARRIGA-ORDONEZ F, NAVA-ALONSO F, URIBE-SALAS A. Cyanide oxidation by ozone in a steady-state flow bubble column [J]. *Minerals Engineering*, 2006, 19: 117–122.
- [14] MOUSSAVI G, MAJIDI F, FARZADKIA M. The influence of operational parameters on elimination of cyanide from wastewater using the electrocoagulation process [J]. *Desalination*, 2011, 280: 127–133.
- [15] DASH R R, GAUR A, BALOMAJUMDER C. Cyanide in industrial wastewaters and its removal: A review on biotreatment [J]. *Journal of Hazardous Materials*, 2009, 163: 1–11.
- [16] OGUTVEREN Ü B, TORU E, KOPARAL S. Removal of cyanide by anodic oxidation for wastewater treatment [J]. *Water Research*, 1999, 33: 1851–1856.
- [17] CHENG S C, GATTRELL M, GUENA T, MACDOUGALL B. The electrochemical oxidation of alkaline copper cyanide solutions [J]. *Electrochim. Acta*, 2002, 47: 3245–3256.
- [18] LOPEZ-MUNOZ M J, AGUADO J, van GRIEKEN R, MARUGAN J. Simultaneous photocatalytic reduction of silver and oxidation of cyanide from dicyanoargentate solutions [J]. *Applied Catalysis B: Environmental*, 2009, 86: 53–62.
- [19] YAZICI E Y, DEVECI H, ALP A. Treatment of cyanide effluents by oxidation and adsorption in batch and column studies [J]. *Journal of Hazardous Materials*, 2009, 166: 1362–1366.
- [20] BEHNAMFRAD A, SALARIRAD M M. Equilibrium and kinetic studies on free cyanide adsorption from aqueous solution by activated carbon [J]. *Journal of Hazardous Materials*, 2009, 170: 127–133.
- [21] WILLIAMS N C, PETERSEN F W. The optimization of an impregnated carbon system to selectively recover cyanide from dilute solutions [J]. *Minerals Engineering*, 1997, 10: 483–490.
- [22] ZHANG Wei, LIU Wan-dong, LV Yan, LI Bing-jing, YING Wei-chi. Enhanced carbon adsorption treatment for removing cyanide from coking plant effluent [J]. *Journal of Hazardous Materials*, 2010, 184: 135–140.
- [23] AHUMADA E, LIZAMA H, ORELLANA F, RODRIGUEZ-REINOSO F. Catalytic oxidation of Fe(II) by activated carbon in the presence of oxygen [J]. *Carbon*, 2002, 40: 2827–2834.
- [24] GIRALDO L, MORENO-PIRAJÁN J C. Adsorption studies of cyanide onto activated carbon and γ -alumina impregnated with copper ions [J]. *Natural Science*, 2010, 2(10): 1066–1072.
- [25] NSAIF ABBAS M, SAEED ABBAS F, ANWER I S. Cyanide removal from wastewater by using banana peel [J]. *Journal of Asian Scientific Research*, 2014, 4(5): 239–247.
- [26] HANG C, CHENG W P. Thermodynamics parameters of iron-cyanide adsorption onto gamma Al₂O₃ [J]. *Journal of Colloid and Interface Science*, 1997, 188: 647–648.
- [27] VEDULA R K, BALOMAJUMDER C. Simultaneous adsorptive removal of cyanide and phenol from industrial wastewater: Optimization of process parameters [J]. *Research Journal of Chemical Sciences*, 2011, 1: 30–39.
- [28] YANG Ji-min, ZHANG Wei, LIU Qing, SUN Wei-yin. Porous ZnO and ZnO–NiO composite nano/microspheres: Synthesis, catalytic and biosensor properties [J]. *RSC Advances*, 2014, 4: 51098–51104.
- [29] GHAEDI M, ANSARI A, HABIBI M H, ASGHARI A R. Removal of malachite green from aqueous solution by zinc oxide nanoparticle loaded on activated carbon: Kinetics and isotherm study [J]. *Journal of Industrial and Engineering Chemistry*, 2014, 20(1): 17–28.
- [30] KUMAR D, KAPOOR I P S, SINGH G, SIRIL P F, TRIPATHI A M. Preparation, characterization, and catalytic activity of nanosized NiO and ZnO: Part 74 [J]. *Propellants, Explosives, Pyrotechnics*, 2011, 36: 268–272.
- [31] DEORE M K, GAIKWAD V B, PATIL R L, PAWAR N K, SHINDE S D, JAIN G H. Effect of Ni doping on gas sensing performance of ZnO thick film resistor [J]. *Sensors & Transducers Journal*, 2010, 122(11): 143–157.
- [32] WOO H S, KWAK C H, CHUNG J H, LEE J H. Highly selective and sensitive xylene sensors using Ni-doped branched ZnO nanowire networks [J]. *Sensors and Actuators, B: Chemical*, 2015, 216(9): 358–366.
- [33] GASPERA D, MARTUCCI E, MICHAEL A. ZnO–NiO thin films containing Au nanoparticles for CO optical sensing [J]. *Sensor Letters*, 2011, 9(2): 600–604.
- [34] XU Lin, ZHENG Rui-fang, LIU Shu-hai, SONG Jian, CHEN Jian-sheng, DONG Biao, SONG Hong-wei. NiO@ZnO hetero structured nanotubes: Coelectrospinning fabrication, characterization, and highly enhanced gas sensing properties [J]. *Inorganic Chemistry*, 2012, 51(14): 7733–40.
- [35] SRIDEVI D, VRAJENDRAN K. Synthesis and optical characteristics of ZnO nanocrystals [J]. *Bulletin of Materials Science*, 2009, 32(2): 165–168.
- [36] EL-KEMARY M A, NAGY N, EL-MEHASSEB I. Nickel oxide

- nanoparticles: Synthesis and spectral studies of interactions with glucose [J]. *Materials Science in Semiconductor Processing*, 2013, 16: 1747–1752.
- [37] SHERLY E, VIJAYA J J. Visible light induced photocatalytic degradation of 2,4-dichlorophenol on ZnO–NiO coupled metal oxides [J]. *International Journal of ChemTech Research*, 2014–2015, 7(3): 1369–1376.
- [38] MAHMOUD A M, IBRAHIM F A, SHABAN S A, YOUSSEF N A. Adsorption of heavy metal ion from aqueous solution by nickel oxide nano catalyst prepared by different methods [J]. *Egyptian Journal of Petroleum*, 2015, 24: 27–35.
- [39] MARDANI H R, FOROUZANI M, ZIARI M, MALEKZADEH A, BIPARVA P. A comparative study of catalytic properties of ZnO and FeZnO nanoparticles on oxidation of benzylic alcohols: Influence of doped metal [J]. *Iranian Chemical Communication*, 2015, 3: 199–207.
- [40] WOO H J, MAJID S, AROF A K. Conduction and thermal properties of a proton conducting polymer electrolyte based on poly (ϵ -caprolactone) [J]. *Solid State Ionics*, 2011, 199–200: 14–20.
- [41] AL-MUSTAFA J. FTIR investigation of the conformational properties of the cyanide bound human hemoglobin [J]. *Vibrational Spectroscopy*, 2002, 30(2): 139–146.
- [42] HASHEMIAN S, FOROGHIMOQHADAM A. Effect of copper doping on CoTiO₃ Ilmenite type nano particles for removal of Congo red from aqueous solution [J]. *Chemical Engineering Journal*, 2014, 235: 299–306.
- [43] HASHEMIAN S, MIRSHAMSI M. Kinetic and thermodynamic of adsorption of 2-picoline by sawdust from aqueous solution [J]. *Journal of Industrial Engineering Chemistry*, 2012, 18: 2010–2015.
- [44] LAGERGREN S. About the theory of so-called adsorption of soluble substances [J]. *Kungliga Svenska Vetenskapsakademiens Handlingar*, 1898, 24: 1–39.
- [45] HO Y S, MCKAY G. The kinetics of sorption of basic dyes from aqueous solution by sphagnum moss peat [J]. *Canadian J Chem Eng*, 1998, 76: 822–827.
- [46] HO Y, MCKAY G. Pseudo-second order model for sorption process [J]. *Chemical Engineering Journal*, 1998, 70: 115–124.
- [47] HASHEMIAN S, SAFFARI H, RAGABION S. Adsorption of cobalt (II) from aqueous solutions by bentonite and Fe₃O₄/bentonite nano composite [J]. *Water Air Soil Pollutant*, 2015, 226: 2212–2221.
- [48] DOGAN M, ALKAN M, TÜRKYILMAZ A, ÖZDEMİR Y. Kinetics and mechanism of removal of methylene blue by adsorption onto perlite [J]. *Journal of Hazardous Materials*, 2004, 109: 141–148.
- [49] IQBAL M J, ASHIQ M N. Adsorption of dyes from aqueous solutions on activated charcoal [J]. *Journal of Hazardous Materials*, 2007, 139: 57–66.
- [50] DADFARNIA S, HAJI SHABANIA A M, MORADIA S E, EMAMI S. Methyl red removal from water by iron based metal-organic frameworks loaded onto iron oxide nanoparticle adsorbent [J]. *Applied Surface Science*, 2015, 330: 85–93.
- [51] ERTUGAY M F, CERTEL M, GURSES A. Moisture adsorption isotherms of Tarhana at 25 °C and 35 °C and the investigation of fitness of various isotherm equations to moisture sorption data of Tarhana [J]. *Journal of the Science of Food and Agriculture*, 2000, 80(14): 2001–2004.
- [52] BARAKAT M A, CHENG Y T, HUANG C P. Removal of toxic cyanide and Cu (II) ions from water by illuminated TiO₂ catalyst [J]. *Applied Catalysis B: Environmental*, 2004, 53: 13–20.
- [53] ASGARI G, MOHAMMADI A S, POORMOHAMMADI A, AHMADIAN M. Removal of cyanide from aqueous solution by adsorption onto bone charcoal [J]. *Fresenius Environmental Bulletin*, 2014, 23(3): 720–727.
- [54] RAMAVANDI B, BARIKBIN B, ASGARI G, GHAEDI H. Efficacy evaluation of activated carbon prepared from date stones in cyanide adsorption from synthetic wastewater [J]. *Journal of Birjand University of Medical Sciences*, 2013, 19(4): 399–408.
- [55] NAEEM S, ZAFAR U. Adsorption studies of cyanide (CN)⁻ on alumina [J]. *Pak Journal Analytical Environmental Chemistry*, 2009, 10(1,2): 83–87.
- [56] AGARWAL B, BALOMAJUMDAR C. Simultaneous adsorption and biodegradation of phenol and cyanide in multicomponent system [J]. *International Journal of Environmental Engineering and Management*, 2013, 4(3): 233–238.

ZnO@NiO 纳米晶粒吸附去除氰化物的动力学和热力学

Mysam PIRMORADI¹, Saeedeh HASHEMIAN¹, Mohammad Reza SHAYESTEH²

1. Department of Chemistry, Islamic Azad University, Yazd branch, Yazd, Iran;

2. Department of Power and Electronic, Faculty of Engineering, Islamic Azad University, Yazd branch, Yazd, Iran

摘要: 合成了 ZnO、NiO 和 ZnO@NiO 纳米晶粒, 采用红外光谱(FTIR)、X 射线衍射(XRD)和扫描电镜(SEM)技术对其进行表征。ZnO、NiO 和 ZnO@NiO 的平均颗粒尺寸为 32、50 和 48 nm。对这些纳米晶粒去除氰化物的能力进行了测定。实验结果表明, 与 ZnO 和 NiO 相比较, ZnO@NiO 纳米晶粒去除氰化物的能力更强。ZnO@NiO 纳米晶粒对氰化铁的去除能力比对氰化钠的更高。研究了反应时间、溶液 pH 值(2~12)、纳米晶粒用量(0.02~0.4 g)和氰化物浓度(5~50 mg/L)等参数对氰化物去除效果的影响。在最优条件下: pH<5, 纳米晶粒用量 0.2 g, 反应时间 30 min, ZnO@NiO 纳米晶粒对 20 mg/L 氰化物的去除率可达到 90%以上。ZnO@NiO 纳米晶粒对氰化物的吸附去除动力学影响规律符合 Langmuir 准二级吸附动力学模型($k_2=4.66\times 10^{-2}$, $R=0.999$)。热力学研究表明, 25 °C 下, 反应的标准焓变化为 7.87 kJ/mol, 自由能变化为 -18.62 kJ/mol。纳米晶粒对氰化物的吸附是一个吸热的自发过程。ZnO@NiO 纳米晶粒是一种能有效去除水或废水中氰化物的吸附剂。

关键词: 氰化物去除; 纳米晶粒; 吸附; ZnO@NiO

(Edited by Sai-qian YUAN)